Published in final edited form as:

Genesis. 2016 August ; 54(8): 447–454. doi:10.1002/dvg.22954.

A knock-in allele of *En1* expressing Dre recombinase

Nicholas W. Plummer, **Jacqueline de Marchena**[2], and **Patricia Jensen**[1]

Neurobiology Laboratory, National Institute of Environmental Health Sciences, National Institutes of Health, Department of Health and Human Services, Research Triangle Park, North Carolina 27709, USA

Abstract

En1 is a homeobox-containing transcription factor expressed during development in diverse tissues, including the embryonic midbrain and anterior hindbrain. To facilitate investigation of genetic and developmental heterogeneity among cells with a history of *En1* expression, we have generated $En1^{Dre}$, a knock-in allele expressing Dre recombinase. $En1^{Dre}$ can be used with existing Cre and Flp recombinase lines for genetic intersectional labeling, fate mapping, and functional manipulation of subpopulations of cells characterized by transient expression of *En1*. To avoid disrupting *En1* function, the Dre cDNA is inserted at the 3′ end of the *En1* coding sequence, together with a viral 2A peptide to mediate translation of separate EN1 and Dre proteins. Consequently, viable and fertile $En1^{Dre}$ homozygotes can be used to increase the proportion of useful genotypes produced in complex crosses. The pattern of Dre expression from $En1^{Dre}$ is indistinguishable from wild-type *En1* expression in mid-gestation mouse embryos, and $En1^{Dre}$ controls Dre-responsive indicator alleles by efficiently recombining rox sites *in vivo*. Through the application of genetic tools that allow manipulation of cells based on combinatorial expression of multiple distinct recombinases, $En1^{Dre}$ will significantly extend the ability to target important subpopulations of neurons and other cells within the broader *En1* expression domain.

Keywords

Dre/rox; mouse; midbrain; hindbrain; recombination

INTRODUCTION

The homeobox-containing transcription factor *Engrailed 1* (*En1*) is expressed during development of a variety of structures, including the limb bud, somites, and central nervous system (Davidson *et al.*, 1988; Davis and Joyner, 1988). In the embryonic mouse brain, *En1* expression is observed at ~E8.5–E9.5 in a region encompassing the midbrain and rhombomere 1 of the anterior hindbrain (Davidson *et al.*, 1988; Davis and Joyner, 1988; McMahon *et al.*, 1992). This complex domain gives rise to anatomically and functionally diverse cell types in the adult, including important subpopulations of dopaminergic, serotonergic, and noradrenergic neurons (Jensen *et al.*, 2008; Robertson *et al.*, 2013; Simon

[1]Correspondence should be addressed to Patricia Jensen, 111 TW Alexander Driver, Box F1-11, Research Triangle Park, NC 27709, USA. Patricia.jensen@nih.gov. (919) 541-0379.

[2]Current address: Impact Pharmaceutical Services, Inc., Durham, NC 27709

et al., 2001; Zervas *et al.*, 2004). Although *En1* expression persists to adulthood in dopaminergic neurons of the substantia nigra and ventral tegmental area (Simon *et al.*, 2001), expression in most midbrain/hindbrain neurons is transient. Therefore, gaining experimental access to these neurons in the mature brain requires the use of recombinase-based strategies (reviewed in Jensen and Dymecki, 2014) to permanently label cells on the basis of transient *En1* expression. A key to this approach is the generation and characterization of transgenic or knock-in alleles which express a site specific recombinase under control of the *En1* promoter, and to date, all such alleles have utilized Cre recombinase (Kimmel *et al.*, 2000; Sapir *et al.*, 2004; Sgaier *et al.*, 2005). Access to some of the distinct neuronal subtypes within the broad *En1* expression domain has been achieved through the use of genetic intersectional strategies (Awatramani *et al.*, 2003), in which subpopulations of cells were defined by overlapping expression of $En1^{Cre}$ and a second recombinase controlled by a different gene promoter (Jensen *et al.*, 2008; Robertson *et al.*, 2013). Because the vast majority of all characterized recombinase driver lines also express Cre, however, applying intersectional strategies to the midbrain and hindbrain requires the generation of new recombinase drivers, to be used in conjunction with $En1^{Cre}$, for each neuronal subtype of interest. Generation of an *En1* allele expressing a recombinase other than Cre would permit the use of existing Cre drivers for intersectional targeting, reducing the need for laborious characterization of new recombinase driver lines and opening new avenues of investigation in the midbrain and hindbrain.

Here, we describe a new *En1* knock-in allele ($En1^{Dre}$) that expresses Dre recombinase (Anastassiadis *et al.*, 2009; Sauer and McDermott, 2004) instead of Cre. Several features of this new allele will make it particularly useful for gaining experimental access to neuronal subpopulations within the complex midbrain/hindbrain *En1* expression domain. $En1^{Dre}$ is compatible with a recently described fluorescent indicator allele (Plummer *et al.*, 2015) that is responsive to three different recombinases (Dre, Flp, and Cre), rendering it useful for investigation of genetic and developmental heterogeneity among *En1*-expressing cell populations that were previously defined using single- or dual-recombinase strategies (Jensen *et al.*, 2008; Robertson *et al.*, 2013; Simon *et al.*, 2001; Zervas *et al.*, 2004). Unlike the existing $En1^{Cre}$ knock-in alleles (Kimmel *et al.*, 2000; Sapir *et al.*, 2004; Sgaier *et al.*, 2005), the Dre insertion in $En1^{Dre}$ does not disrupt *En1* expression. Therefore, $En1^{Dre}$ mice can be bred to homozygosity, increasing the percentage of experimentally useful offspring in the complex crosses required for intersectional analyses. We have confirmed that Dre expression copies endogenous *En1* expression in mid-gestation embryos, when *En1* expression is most widespread. Furthermore, Dre levels in $En1^{Dre}$ heterozygotes are sufficient to efficiently recombine rox target sites in Dre-responsive indicator alleles. Thus, $En1^{Dre}$ will be a valuable tool for analysis of neurons in the midbrain/hindbrain and *En1*-expressing cells elsewhere in the embryo.

RESULTS AND DISCUSSION

To express Dre recombinase under control of the *En1* promoter without disrupting *En1* transcription or translation, we used a 2A peptide derived from *Thosea asigna* virus, which permits expression of two separate polypeptides from a single mRNA (Donnelly *et al.*, 2001; Trichas *et al.*, 2008). A construct consisting of the 2A peptide sequence, mammalian codon-

optimized Dre cDNA (Anastassiadis *et al.*, 2009), and SV40 poly(A) cassette was targeted to exon 2 of the mouse *En1* gene by homologous recombination in embryonic stem cells. This construct replaces the stop codon and 41 bp of the 3′ UTR without altering the coding sequence of *En1* (Fig. 1). Mice homozygous for the new $En1^{Dre}$ allele are viable and fertile, without the perinatal lethality and developmental defects associated with mutation of *En1* (Wurst *et al.*, 1994), indicating that the 2A-Dre-poly(A) insertion does not disrupt *En1* function.

In the mouse embryo, *En1* expression has been detected in the neural plate at the 1-somite stage (~E8.0) and by E8.5/E9.0 is observed in the midbrain and anterior hindbrain (Davis and Joyner, 1988; McMahon *et al.*, 1992). By E12, expression can be observed in a variety of other tissues, including spinal cord, somites, and limb bud (Davidson *et al.*, 1988; Davis and Joyner, 1988). To confirm that Dre expression recapitulates the wild-type expression pattern of *En1*, we used *in situ* hybridization to detect *En1* and Dre mRNA in sections from $En1^{Dre}$ heterozygotes and littermate control embryos at approximately E9.5 and E11.0. As expected, we observed Dre expression spanning the midbrain/hindbrain junction, and in spinal cord, somites, and limb buds (Fig. 2). The distribution of Dre labeling was indistinguishable from that of *En1*.

The usefulness of $En1^{Dre}$ as a recombinase driver allele depends on its ability to recombine rox sites, the targets of Dre recombinase that are analogous to the loxP target sites of Cre (Sauer and McDermott, 2004). We tested this capability *in vivo* using two Dre-responsive fluorescent indicator alleles, *RC::RG* and *RC::RLTG* (Plummer *et al.*, 2015), which express eGFP or tdTomato, respectively, following Dre-mediated excision of a rox-flanked transcriptional stop cassette. In whole-mount $En1^{Dre}$*; RC::RG* double heterozygous embryos at E10.5 (Fig. 3a–d), we observed eGFP fluorescence in the midbrain/hindbrain, first pharyngeal arch, limb buds, and somites. The pattern of recombination-dependent fluorescence is consistent with the cumulative expression of *En1* by this developmental stage and is very similar to the labeling observed at E10.5 when a Cre-dependent *LacZ* indicator is recombined by $En1^{Cre}$ (http://www.informatics.jax.org/recombinase/specificity?id=MGI:2446434&system=head). No fluorescence was observed in the absence of $En1^{Dre}$ (Fig. 3e–f). In sagittal sections of adult $En1^{Dre}$*; RC::RLTG* double heterozygous brain, tdTomato was observed in midbrain and anterior hindbrain, including the entire cerebellum (Fig. 4a). At higher magnification, recombination appeared complete within the *En1* expression domain, with no unlabeled cells that would indicate mosaic expression or insufficient recombinase activity (Fig. 4b–d). It has been reported that Dre recombinase can interact with loxP sites in some circumstances (Fenno *et al.*, 2014), potentially complicating the use of $En1^{Dre}$ for intersectional analyses. To test this phenomenon, we used the *RC::RLTG* allele, which expresses eGFP following excision of the rox-flanked stop cassette and the loxP-flanked tdTomato-stop cassette (Fig. 4). Thus, eGFP will be expressed in $En1^{Dre}$*; RC::RLTG* brain only if Dre recombines the loxP sites as well as the rox sites. We observed no eGFP labeled cells (n=4 brains), consistent with prior observations that Dre and loxP sites are generally incompatible in transgenic systems (Chuang *et al.*, 2015; Park and Leach, 2013; Plummer *et al.*, 2015), with significant cross-reactivity only observed in the context of viral vector-driven overexpression (Fenno *et al.*, 2014). These results confirm that $En1^{Dre}$ is suitable for use in intersectional genetic analyses together with Cre driver alleles.

This characterization demonstrates that *En1*^{Dre} faithfully recapitulates the wild-type expression pattern of *En1* and efficiently recombines rox sites *in vivo*. Therefore, *En1*^{Dre} is compatible with the diverse Dre-responsive genetic tools and strategies that have been developed in the past several years, including fluorescent indicator alleles responsive to Dre and one or more additional site-specific recombinases (Madisen *et al.*, 2015; Plummer *et al.*, 2015). Because Dre and Cre have different target sites, they can function independently in the same animal. For example, recombination of an indicator allele by *En1*^{Dre} could be used to trace specific cell populations in the context of Cre-dependent conditional mutagenesis of a different gene. Alternatively, Dre-dependent Cre alleles (Hermann *et al.*, 2014; Sajgo *et al.*, 2014) offer the possibility of intersectional control of conditional mutagenesis and Cre-dependent effector alleles. These strategies will provide experimental access to cells with a history of *En1*^{Dre} expression, including those that express *En1* transiently during development. To specifically target cells that express *En1* in the adult, without interference from embryonic *En1* domains, *En1*^{Dre} can be used in conjunction with injection of Dre-responsive and Dre/Cre-responsive viral constructs encoding indicators and effectors (Chuang *et al.*, 2015; Fenno *et al.*, 2014; Madisen *et al.*, 2015). Several of these recently described constructs utilize engineered mutant rox target sites to permit control of indicator or effector gene expression by Dre-dependent inversion and excision similar to Cre-dependent FLEx/DIO constructs (Chuang *et al.*, 2015; Fenno *et al.*, 2014). Given these possibilities, we expect that *En1*^{Dre} will become an important part of the genetic toolbox for analysis of neurons in the mammalian midbrain and hindbrain.

METHODS

Generation of En1^{Dre} mice

To generate the *En1*^{Dre} targeting vector, we first used pCAGGS-Dre-IRES-Puro (Anastassiadis *et al.*, 2009) as template to amplify a mammalian codon-optimized Dre cDNA lacking the start codon. We used the primers 5′-CAGTACTAGTGGCAGTGGAGAGGGCAGAGGAAGTCTGCTAACATGCGGTGACGTCGAGGAGAATCCTGGCCCAATGGGTGCTAGCGAGCTGAT, which contains the 2A peptide (underlined), and 5′-CAGTCTGCAGTTATCACACTTTCCTCTTCTTCTTAGGACCG. The PCR product was cloned into pGEM-5Z (Clontech Laboratories, Mountain View, CA), using the SpeI and PstI sites included in the primers, to generate pGEM-2ADre. The SV40 poly(A) cassette was amplified from pBS302 (Addgene plasmid #11925) (Sauer, 1993) using primers 5′-CAGTCTGCAGGATCATAATCAGCCATACCA and 5′-CAGTGTCGACGATCCAGACATGATAAGATA and cloned between the PstI and SalI sites of pGEM-2ADre to generate pGEM-2ADre-stop. A 469 bp fragment of *En1* intron 1 and exon 2 ending immediately before the stop codon was amplified using primers 5′-CAGTGGGCCCAGCAGCTGGCCTCTACAATC and 5′-CAGTACTAGTCTCGCTCTCGTCTTTGTCCT and cloned between the ApaI and SpeI sites upstream of the 2A peptide in pGEM-2ADre-stop. Primers 5′-CAGTGTCGACGGTGCCAGGGCGTGCCCTTGGGCTCCCCGGGCGCGTTAGGTCTGAAGAGGAGTTT and 5′-CAGTCATATGCAGTCCTAGGCCCCCAACTGAGAGAACTCAAAGGTTACCCCAGTT

GGGGATTAAGGGTTCCGCAAGCTCT containing attB35 and attP39B sites, respectively (underlined) (Groth *et al.*, 2000) were used to amplify a neomycin resistance gene with both PGK and Em7 promoters from PL452 (Liu *et al.*, 2003). The attB- attP-flanked neomycin cassette was cloned between the SalI and NdeI sites downstream of the Sv40 poly(A) cassette. 497 bp of *En1* 3′UTR was amplified with primers 5′-CAGTCCTAGGGTGCCACCTCCAGGCTCCTC and 5′-CAGTCATATGGGTGCAGGAGGTACCCAGAG and cloned using the AvrII and NdeI sites adjacent to the Neo Cassette. After the resulting plasmid was digested with ApaI and NdeI, the two fragments of *En1* served as targets for homologous recombination with bacterial artificial chromosome (BAC) RP23-488D12 in *E. coli* strain DY380 (Lee *et al.*, 2001). To generate the final targeting vector from the recombinant BAC, a 12.5 KB fragment consisting of 4.4 KB 5′ homology arm, 2ADre-Neo cassette, and 4.9 KB 3′ homology arm was retrieved into pL253 (Liu *et al.*, 2003) by homologous recombination in DY380 cells. For linearizing the vector, an AscI site was added at the 3′ end of the 3′ homology arm.

Linearized targeting vector DNA was electroporated into G4 embryonic stem cells (B6129 F1 genetic background). Homologous recombinants were identified by long range PCR using the Expand Long Range dNTP Pack (Roche Applied Science) and primers specific for the 5′and 3′ ends of each recombinant locus. Southern blots probed for the neomycin resistance gene were used to confirm absence of random integrations. The karyotypes of recombinant clones were assessed, and several clones were transfected with pPGKPhiC31obpa (Raymond and Soriano, 2007) to remove the Neo cassette. The clones were then injected into blastocysts of B6(Cg)-*Tyr*$^{c\text{-}2J}$/J mice to produce chimeric mice, and male chimeras were bred to female C57BL/6J mice to establish the *En1*^{Dre} mouse line. *En1*^{Dre} mice will be available to the research community upon publication of this manuscript.

Experimental crosses

En1^{Dre} mice were maintained as heterozygotes by back-crossing to C57BL/6J mice or as homozygotes by intercrossing. For assessment of *in vivo* recombination, *En1*^{Dre} heterozygotes were crossed with *Gt(ROSA)26Sor*$^{tm1.2(CAG\text{-}tdTomato,\ \text{-}EGFO)Pjen}$ (*RC::RLTG*) and *RC::RG* mice (Plummer *et al.*, 2015). All mouse experiments were performed with approval of the National Institute of Environmental Health Sciences (NIEHS) Institutional Animal Care and Use Committee.

Tissue collection

Embryos were fixed by immersion overnight at 4 °C in 4% paraformaldehyde (PFA) diluted in 0.01 M phosphate buffered saline (PBS). Adult mice were anesthetized with sodium pentobarbital and perfused transcardially with 4% PFA in PBS. After dissection, brains were post-fixed overnight by immersion in 4% PFA in PBS at 4 °C, rinsed in PBS, and equilibrated in 30% sucrose diluted in PBS at 4 °C for 48 hours. Embryos were equilibrated in 10%, 20%, and finally 30% sucrose diluted in PBS. The cryoprotected samples were then embedded in Tissue Freezing Medium (General Data Company, Cincinnati, OH) and sectioned on a Leica CM3050 S cryostat (Leica Biosystems, Buffalo Grove, IL). After sectioning, 40-μm thick free floating brain sections were stored at −80 °C in a solution of

30% sucrose and 30% ethylene glycol in PBS. For embryos, 14-μm thick sections were mounted on Superfrost Plus microscope slides (Thermo Scientific, Waltham, MA), air dried, and stored at −80 °C.

In situ hybridization

RNA *in situ* hybridization using RNAscope technology (Wang *et al.*, 2012) was performed on 14-μm thick embryo sections according to the manufacturer's instructions for the RNAscope 2.5 HD Reagent Kit-Red (Advanced Cell Diagnostics, Hayward, CA). Probes used were En1 (Cat# 442651, Advanced Cell Diagnostics) and a custom Dre probe (Cat# 442641, Advanced Cell Diagnostics) raised against nucleotides 83-999 of the mammalian codon-optimized Dre coding sequence (Anastassiadis *et al.*, 2009). Hybridized RNA was detected with Fast Red dye, and tissue was counterstained with hematoxylin.

Immunohistochemistry

Immunofluorescent labeling was performed on 40-μm free floating sagittal brain sections from adult mice. tdTomato-expressing cells were labeled by rabbit anti-dsRed primary antibody (1:1000; Cat.# 632496, Clontech Laboratories, Mountain View, CA) and Alexa Fluor 568 goat anti-rabbit secondary antibody (1:1000; Cat.# A11036, Life Technologies, Grand Island, NY). To test for possible eGFP expression resulting from Dre-dependent recombination of loxP sites in *RC::RLTG*, we used chicken anti-GFP primary antibody (1:10,000; Cat.# ab13970, Abcam, Cambridge MA) and Alexa Fluor 488 goat anti-chicken secondary antibody (1:1000; Cat.# A11039, Life Technologies). After immunolabeling, sections were mounted on microscope slides, and coverslips were attached with Vectashield plus DAPI (Vector Laboratories, Burlingame, CA). Every fourth section across the entire brain was stained and examined.

Imaging

Images of embryo sections labeled by *in situ* hybridization were collected on an Olympus IX70 inverted microscope (Olympus Corporation, Center Valley, PA), and images of whole mount embryos were collected on a Zeiss SterREO Lumar.V12 stereomicroscope (Carl Zeiss Microscopy, Thornwood, NY). Immunolabeled sagittal sections of adult brain were imaged on a Zeiss LSM 780 inverted confocal microscope. Tile images of the entire section were digitally stitched and confocal z-stacks were converted to maximum intensity projections using Zen 2012 Black Software (Carl Zeiss). Images were then imported into Photoshop Software (Adobe Systems, San Jose, CA) and modified only by adjusting the brightness and contrast of the entire image.

Acknowledgments

NIH Support: This research was supported by the Intramural Research Program of the US National Institutes of Health, National Institute of Environmental Health Sciences (ES102805).

We thank D. D'Agostin, G. Jones, and K. Smith for technical assistance. We thank F. Stewart (Technische Universität Dresden) for the Dre cDNA. Valuable support was provided by the NIEHS Comparative Medicine Branch, Knockout Mouse Core, and Fluorescence Microscopy and Imaging Core. This research was supported by the Intramural Research Program of the US National Institutes of Health, National Institute of Environmental Health Sciences (ES102805).

References

Anastassiadis K, Fu J, Patsch C, Hu S, Weidlich S, Duerschke K, Buchholz F, Edenhofer F, Stewart AF. Dre recombinase, like Cre, is a highly efficient site-specific recombinase in E. coli, mammalian cells and mice. Dis Model Mech. 2009; 2:508–515. [PubMed: 19692579]

Awatramani R, Soriano P, Rodriguez C, Mai JJ, Dymecki SM. Cryptic boundaries in roof plate and choroid plexus identified by intersectional gene activation. Nat Genet. 2003; 35:70–75. [PubMed: 12923530]

Chuang K, Nguyen E, Sergeev Y, Badea TC. Novel Heterotypic Rox Sites for Combinatorial Dre Recombination Strategies. G3 (Bethesda). 2015; 6:559–571. [PubMed: 26715092]

Davidson D, Graham E, Sime C, Hill R. A gene with sequence similarity to Drosophila engrailed is expressed during the development of the neural tube and vertebrae in the mouse. Development. 1988; 104:305–316. [PubMed: 2908202]

Davis CA, Joyner AL. Expression patterns of the homeo box-containing genes En-1 and En-2 and the proto-oncogene int-1 diverge during mouse development. Genes Dev. 1988; 2:1736–1744. [PubMed: 2907320]

Donnelly ML, Hughes LE, Luke G, Mendoza H, ten Dam E, Gani D, Ryan MD. The 'cleavage' activities of foot-and-mouth disease virus 2A site-directed mutants and naturally occurring '2A-like' sequences. J Gen Virol. 2001; 82:1027–1041. [PubMed: 11297677]

Fenno LE, Mattis J, Ramakrishnan C, Hyun M, Lee SY, He M, Tucciarone J, Selimbeyoglu A, Berndt A, Grosenick L, Zalocusky KA, Bernstein H, Swanson H, Perry C, Diester I, Boyce FM, Bass CE, Neve R, Huang ZJ, Deisseroth K. Targeting cells with single vectors using multiple-feature Boolean logic. Nat Methods. 2014; 11:763–772. [PubMed: 24908100]

Groth AC, Olivares EC, Thyagarajan B, Calos MP. A phage integrase directs efficient site-specific integration in human cells. Proc Natl Acad Sci U S A. 2000; 97:5995–6000. [PubMed: 10801973]

Hermann M, Stillhard P, Wildner H, Seruggia D, Kapp V, Sanchez-Iranzo H, Mercader N, Montoliu L, Zeilhofer HU, Pelczar P. Binary recombinase systems for high-resolution conditional mutagenesis. Nucleic Acids Res. 2014; 42:3894–3907. [PubMed: 24413561]

Jensen P, Dymecki SM. Essentials of recombinase-based genetic fate mapping in mice. Methods Mol Biol. 2014; 1092:437–454. [PubMed: 24318835]

Jensen P, Farago AF, Awatramani RB, Scott MM, Deneris ES, Dymecki SM. Redefining the serotonergic system by genetic lineage. Nat Neurosci. 2008; 11:417–419. [PubMed: 18344997]

Kimmel RA, Turnbull DH, Blanquet V, Wurst W, Loomis CA, Joyner AL. Two lineage boundaries coordinate vertebrate apical ectodermal ridge formation. Genes Dev. 2000; 14:1377–1389. [PubMed: 10837030]

Lee EC, Yu D, Martinez de Velasco J, Tessarollo L, Swing DA, Court DL, Jenkins NA, Copeland NG. A highly efficient Escherichia coli-based chromosome engineering system adapted for recombinogenic targeting and subcloning of BAC DNA. Genomics. 2001; 73:56–65. [PubMed: 11352566]

Liu P, Jenkins NA, Copeland NG. A highly efficient recombineering-based method for generating conditional knockout mutations. Genome Res. 2003; 13:476–484. [PubMed: 12618378]

Madisen L, Garner AR, Shimaoka D, Chuong AS, Klapoetke NC, Li L, van der Bourg A, Niino Y, Egolf L, Monetti C, Gu H, Mills M, Cheng A, Tasic B, Nguyen TN, Sunkin SM, Benucci A, Nagy A, Miyawaki A, Helmchen F, Empson RM, Knopfel T, Boyden ES, Reid RC, Carandini M, Zeng H. Transgenic mice for intersectional targeting of neural sensors and effectors with high specificity and performance. Neuron. 2015; 85:942–958. [PubMed: 25741722]

McMahon AP, Joyner AL, Bradley A, McMahon JA. The midbrain-hindbrain phenotype of Wnt-1^{-}/Wnt-1^{-} mice results from stepwise deletion of engrailed-expressing cells by 9.5 days postcoitum. Cell. 1992; 69:581–595. [PubMed: 1534034]

Park JT, Leach SD. TAILOR: transgene activation and inactivation using lox and rox in zebrafish. PLoS One. 2013; 8:e85218. [PubMed: 24391998]

Plummer NW, Evsyukova IY, Robertson SD, de Marchena J, Tucker CJ, Jensen P. Expanding the power of recombinase-based labeling to uncover cellular diversity. Development. 2015; 142:4385–4393. [PubMed: 26586220]

Raymond CS, Soriano P. High-efficiency FLP and PhiC31 site-specific recombination in mammalian cells. PLoS One. 2007; 2:e162. [PubMed: 17225864]

Robertson SD, Plummer NW, de Marchena J, Jensen P. Developmental origins of central norepinephrine neuron diversity. Nat Neurosci. 2013; 16:1016–1023. [PubMed: 23852112]

Sajgo S, Ghinia MG, Shi M, Liu P, Dong L, Parmhans N, Popescu O, Badea TC. Dre - Cre sequential recombination provides new tools for retinal ganglion cell labeling and manipulation in mice. PLoS One. 2014; 9:e91435. [PubMed: 24608965]

Sapir T, Geiman EJ, Wang Z, Velasquez T, Mitsui S, Yoshihara Y, Frank E, Alvarez FJ, Goulding M. Pax6 and engrailed 1 regulate two distinct aspects of renshaw cell development. J Neurosci. 2004; 24:1255–1264. [PubMed: 14762144]

Sauer B. Manipulation of transgenes by site-specific recombination: use of Cre recombinase. Methods Enzymol. 1993; 225:890–900. [PubMed: 8231893]

Sauer B, McDermott J. DNA recombination with a heterospecific Cre homolog identified from comparison of the pac-c1 regions of P1-related phages. Nucleic Acids Res. 2004; 32:6086–6095. [PubMed: 15550568]

Sgaier SK, Millet S, Villanueva MP, Berenshteyn F, Song C, Joyner AL. Morphogenetic and cellular movements that shape the mouse cerebellum; insights from genetic fate mapping. Neuron. 2005; 45:27–40. [PubMed: 15629700]

Simon HH, Saueressig H, Wurst W, Goulding MD, O'Leary DD. Fate of midbrain dopaminergic neurons controlled by the engrailed genes. J Neurosci. 2001; 21:3126–3134. [PubMed: 11312297]

Trichas G, Begbie J, Srinivas S. Use of the viral 2A peptide for bicistronic expression in transgenic mice. BMC Biol. 2008; 6:40. [PubMed: 18793381]

Wang F, Flanagan J, Su N, Wang LC, Bui S, Nielson A, Wu X, Vo HT, Ma XJ, Luo Y. RNAscope: a novel in situ RNA analysis platform for formalin-fixed, paraffin-embedded tissues. J Mol Diagn. 2012; 14:22–29. [PubMed: 22166544]

Wurst W, Auerbach AB, Joyner AL. Multiple developmental defects in Engrailed-1 mutant mice: an early mid-hindbrain deletion and patterning defects in forelimbs and sternum. Development. 1994; 120:2065–2075. [PubMed: 7925010]

Zervas M, Millet S, Ahn S, Joyner AL. Cell behaviors and genetic lineages of the mesencephalon and rhombomere 1. Neuron. 2004; 43:345–357. [PubMed: 15294143]

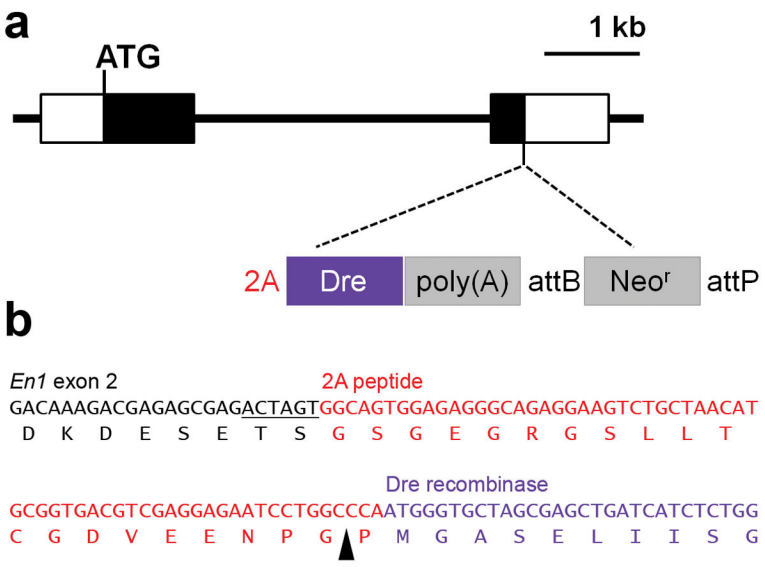

Figure 1. Structure of the *En1*^{Dre} allele

(a) Schematic diagram of the *En1* locus showing insertion site of 2A peptide, Dre cDNA, and Neomycin resistance gene (Neo^r). Black rectangles represent *En1* coding sequence. Unfilled rectangles represent 5′ and 3′ untranslated regions. In *En1*^{Dre} mice, Neo^r has been excised by ϕC31-mediated recombination of the attB and attP sites. (b) Sequence from the *En1*^{Dre} allele showing the junction between *En1* exon 2, 2A peptide, and Dre cDNA. An exogenous SpeI restriction site (underlined) links *En1* exon 2 to the 2A peptide. The black arrowhead indicates the cleavage site within the 2A peptide.

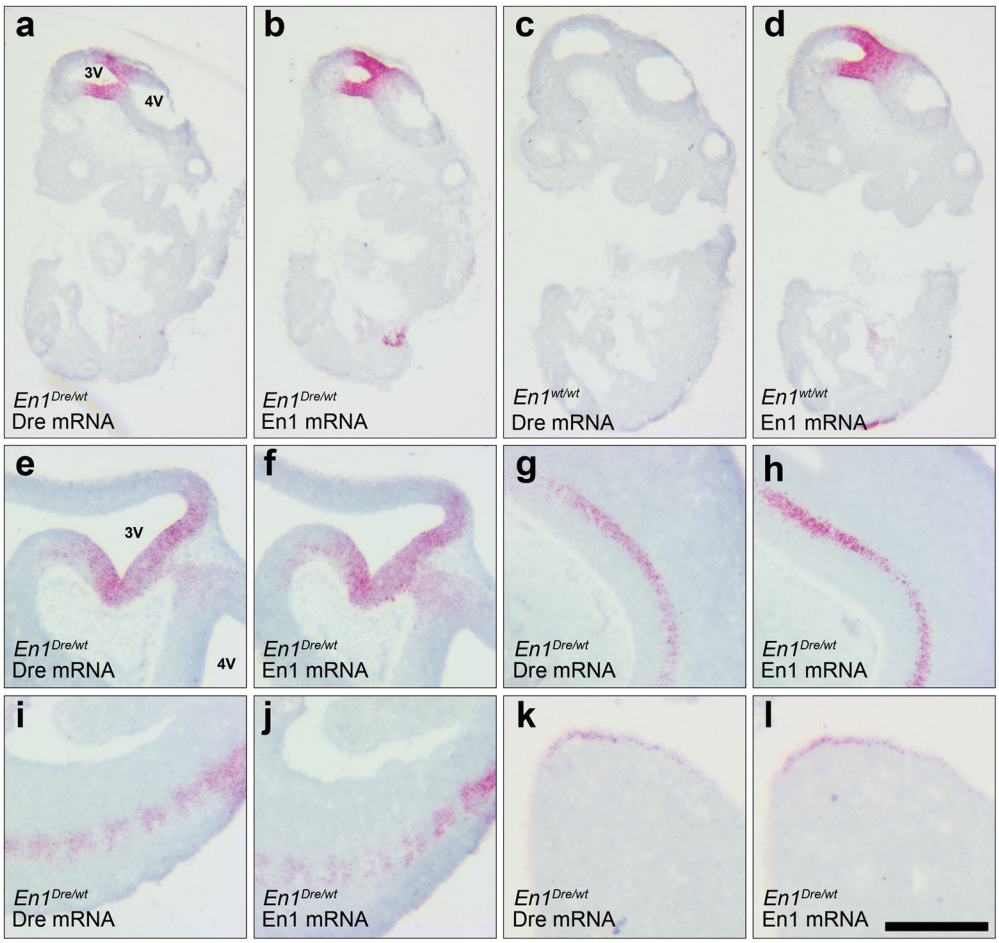

Figure 2. Expression of Dre matches *En1* in mid-gestation embryos

Sagittal sections of E9.5 (a–d) and E11 (e–l) embryos labeled by RNA in-situ hybridization using Dre or *En1* riboprobes. In an $En1^{Dre}$ heterozygous embryo at E9.5, Dre expression at the midbrain/hindbrain junction (a) matches expression of *En1* (b). In a wild-type embryo (c–d), only *En1* expression is observed, confirming specificity of the Dre riboprobe. At E11, Dre and *En1* expression patterns are indistinguishable at the midbrain/hindbrain junction (e–f) and in spinal cord (g–h), somites (i–j), and hindlimb bud (k–l). 3V, third ventricle; 4V, fourth ventricle. Scalebar: 645 μm (a–d), 500 μm (e–j), or 250 μm (k–l).

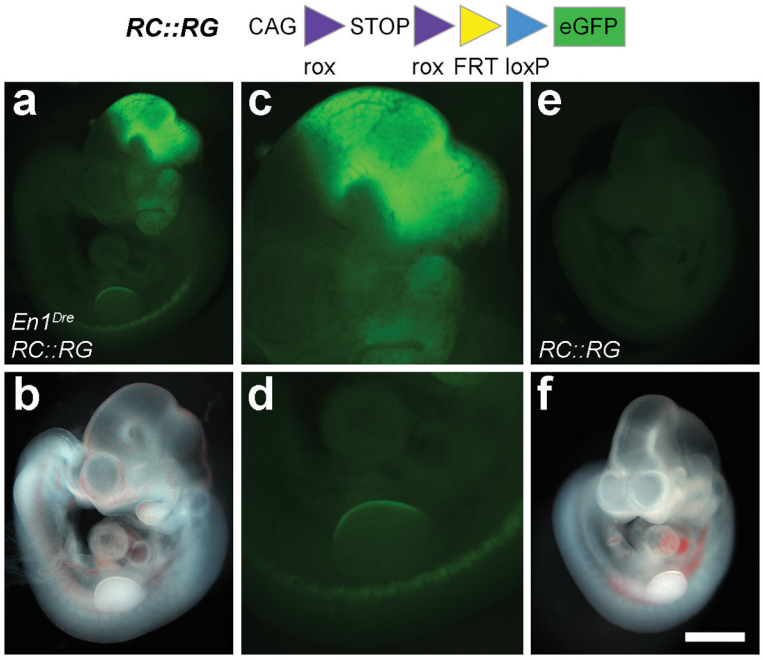

Figure 3. *En1*^{Dre} efficiently recombines a Dre-responsive indicator allele in mouse embryos

Fluorescence (a, c–e) or brightfield (b, f) images of a whole-mount *En1*^{Dre}*; RC::RG* double heterozygous embryo (a–d) and a Dre-negative littermate control (e–f) at E10.5. eGFP fluorescence, indicating recombination of the rox-flanked transcriptional stop cassette, is visible in midbrain/hindbrain (a, c), first pharyngeal arch (a), somites (a, d), and forelimb bud (a, d) of the double heterozygote. No fluorescence is observed in the control embryo (e). Images show native fluorescence. Scalebar: 1000 μm (a–b, e–f); 458 μm (c–d).

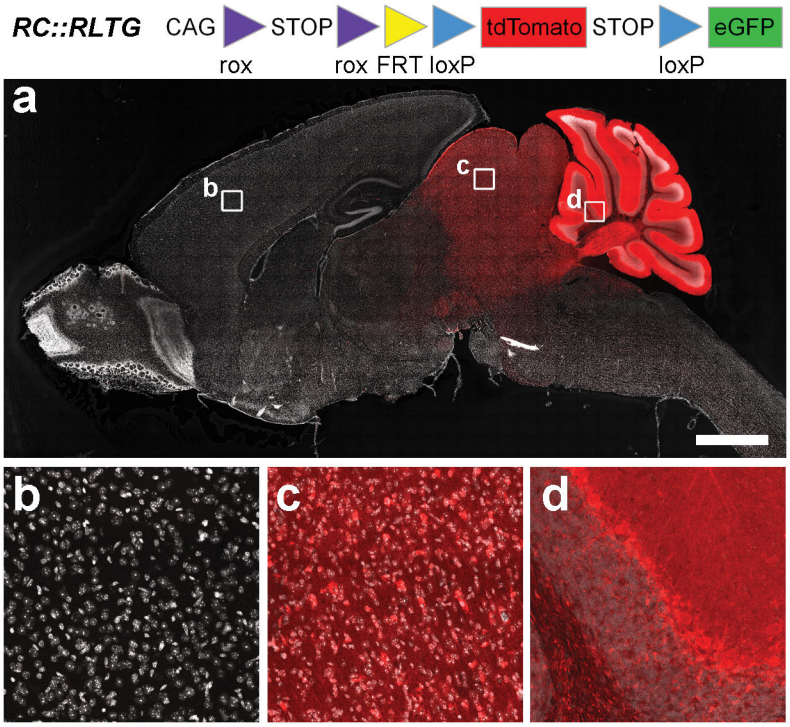

Figure 4. *En1*^{Dre} can be used to trace cells with a history of embryonic *En1* expression into the adult brain

Sagittal section of adult brain from an *En1*^{Dre}*; RC:RLTG* double heterozygote. tdTomato expression, indicating recombination of the rox-flanked stop cassette, is restricted to cells derived from embryonic midbrain and rhombomere 1 of the anterior hindbrain. Nuclear DAPI staining (false-colored gray) reveals tissue that does not express tdTomato (a, b). At higher magnification, recombination appears complete, with no unlabeled cells observed in superior colliculus (c) and cerebellum (d). Images show immunofluorescence. Scalebar: 2000 μm (a) or 97 μm (b–d).